Numerical analysis of elastic vibration of superconducting maglev vehicles

H. Ohsaki & S. Bando
The University of Tokyo, Kashiwa, Japan

ABSTRACT: This paper describes elastic body models of superconducting maglev vehicles for numerical analysis of vehicle dynamics and riding comfort. Elastic cylindrical beam models are presented, and some analysis results of vehicle dynamics of the maglev train by using the elastic body model are shown, where the vehicle moves along the straight guideway with imperfections of coil or panel arrangement, or along the curve with a radius of 8,000 m.

1 INTRODUCTION

Running tests of the superconducting maglev vehicles have been performed at the Yamanashi Maglev Test Line since April 1997 (Seki et al 2002). The maglev system recorded the highest speed of 581 km/h and the highest relative speed of 1,026 km/h in the passing test of two maglev trains, and has reached the technically practical phase as an ultra high-speed mass transport. Further development and evaluation tests have been being carried out to improve the system.

The superconducting maglev system is based on the electrodynamic suspension (EDS) (Fujiwara & Fujimoto 1989) and the propulsion by linear synchronous motors (LSM), where superconducting coils on the bogies interact with ground coils, as shown in Figure 1. The maglev train can travel in stable levitation state at speeds above 100-150 km/h with an air gap length of 10 cm.

The authors have carried out numerical analysis of the running characteristics of superconducting maglev vehicles by using a general-purpose mechanical dynamics analysis software combined with a FORTRAN program solving electric circuit equations that describe electromagnetic phenomena in the system, to study the vehicle dynamics and riding comfort (Ohsaki et al. 2000, Early & Ohsaki 2001, Early et al. 2002). On the other hand, in high-speed railways including the superconducting maglev, elastic vibrations caused by lower rigidity of lighter car bodies are observed. For more precise and realistic study of the vehicle dynamics and riding comfort in the superconducting maglev the authors have considered an elastic body model of maglev vehicles.

The elastic cylindrical beam model has been created, which has the bending vibration characteristics similar to the real maglev car body tested at the Yamanashi Maglev Test Line up to the third bending mode, keeping the parameters related to fundamental translation and rotation motions, such as the mass, the moments of inertia, etc.

In this paper, a numerical analysis model and method will be described with an emphasis on how to model an elastic car body, and then elastic vibration characteristics of the superconducting maglev under some perturbation force conditions will be shown.

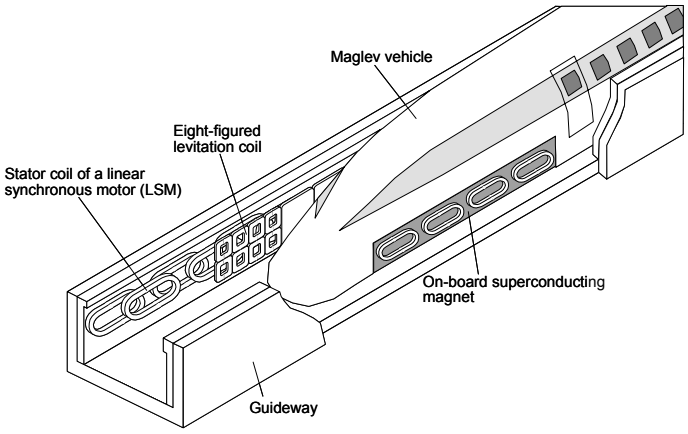

Figure 1: Superconducting maglev system at the Yamanashi Maglev Test Line.

2 ANALYSIS METHOD AND MODEL

2.1 Numerical analysis method

The superconducting maglev system is composed of the mechanical and electromagnetic systems. The mechanical system was modeled and solved by SIMPACK, a multi-body simulation tool, while the electromagnetic system was solved by our self-developed analysis program, which was linked to SIMPACK. Modeling an elastic car body was also performed using analysis tools of SIMPACK.

The electromagnetic system consisting of EDS and LSM is given as an air-core coil system, and modeled as linear electric circuits comprising their resistances, self-inductances and mutual inductances (Ohsaki et al. 2000). At each time step electromagnetic forces and torques acting on superconducting coils are calculated from the superconducting coil currents and ground coil currents, and then forces and torques acting on centers of gravity of bogies and car bodies are transferred to SIMAPCK. Figure 2 shows the numerical calculation flow. The details of calculation method of currents and mutual inductances are described in the previous papers (Ohsaki et al. 2000, Early & Ohsaki 2001, Early et al. 2002).

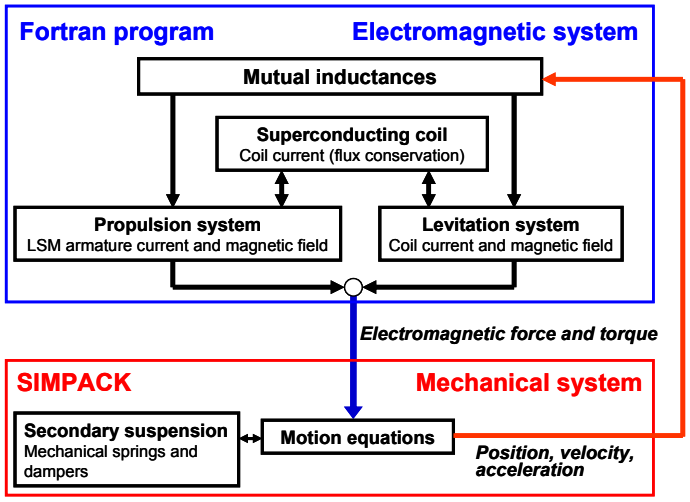

Figure 2: Numerical simulation of vehicle dynamics of a superconducting maglev train composed of electromagnetic and mechanical systems.

2.2 Numerical analysis model

A vehicle model composed of three car bodies and four bogies shown in Figure 3 was used in the numerical analysis. There are two bogies connecting the cars and two bogies on either end. Each bogie has eight superconducting coils, four on each side. Fundamental model parameters were taken from the system at the Yamanashi Maglev Test Line.

For study of the influence of elastic vibration of a car body on vehicle dynamics and riding comfort, an elastic body model has been introduced for a car body. As shown in Figure 4, only the middle car was modeled as an elastic body in this work.

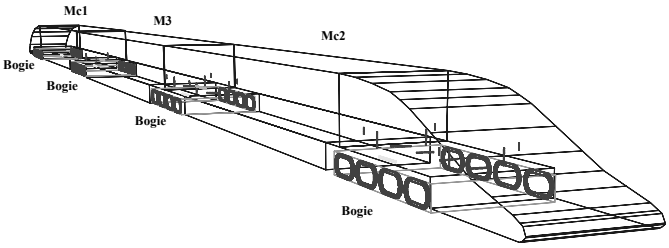

Figure 3: Numerical analysis model for mechanical components of the superconducting maglev system.

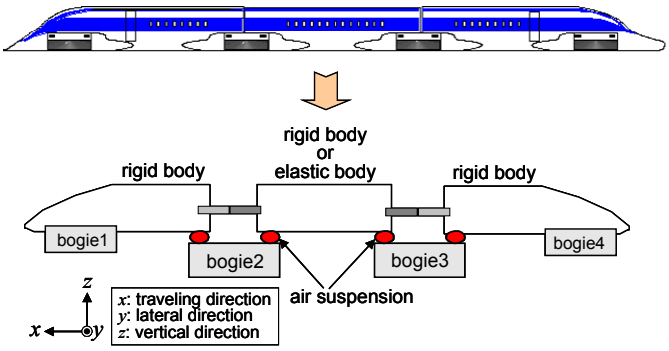

Figure 4: Introduction of an elastic body model for the middle car.

3 ELASTIC BODY MODEL

3.1 Overview

Elastic body models for the middle car are described in this section. A beam model having the bending vibration characteristics similar to the tested middle car was created, keeping the parameters related to fundamental translation and rotation motions, such as the mass, the moments of inertia, the vehicle length, etc. (Ohsaki & Abe 2003)

3.2 Fundamental equation

Displacement of the beam $u(x,t)$ can be obtained from the following fundamental equation with adequate boundary conditions:

$$EI\frac{\partial^4 u(x,t)}{\partial x^4} = \rho A\frac{\partial^2 u(x,t)}{\partial t^2} \qquad (1)$$

where ρ is the mass density, A is the cross section, E is the modulus of longitudinal elasticity or Young's modulus, and I is the geometrical moment of inertia.

When EI is constant, the bending vibration mode frequencies f_n are given by the following equation:

$$f_n = \frac{1}{2\pi}\left(\frac{\alpha_n}{L}\right)^2 \sqrt{\frac{EI}{\rho A}} \quad (n = 1, 2, 3, \cdots) \qquad (2)$$

where α_n is the parameter determined from the support and boundary conditions of the beam, and L is the beam length.

3.3 *Parameter determination*

The fundamental geometrical parameters were given from the existing analysis model used so far, such as the mass, the geometrical moment of inertia, and the vehicle length. From these parameters the additional parameters for a cylindrical beam model were calculated, such as the equivalent diameter and the equivalent cross section. A poison's ratio was assumed to be 0.3. The modulus of longitudinal elasticity was finally determined, so that resultant resonance frequencies of the first and third bending modes could coincide with those obtained in the running test. The following two kinds of analysis models were considered, as shown in Figure 5:

(1) MODEL-1: Uniform cylindrical model
This is the most simple cylindrical beam model. It was assumed that the mass density ρ and the modulus of longitudinal elasticity E were uniform along the cylindrical beam. Only E was the variable parameter in modeling.

(2) MODEL-2: Non-uniform cylindrical model

A distribution of the parameter $K=\rho/E$ was given as shown in Figure 5. The middle car body was modeled with three beam components. The two end components with the length of a and the one middle component with the length of L-2a had different values of K.

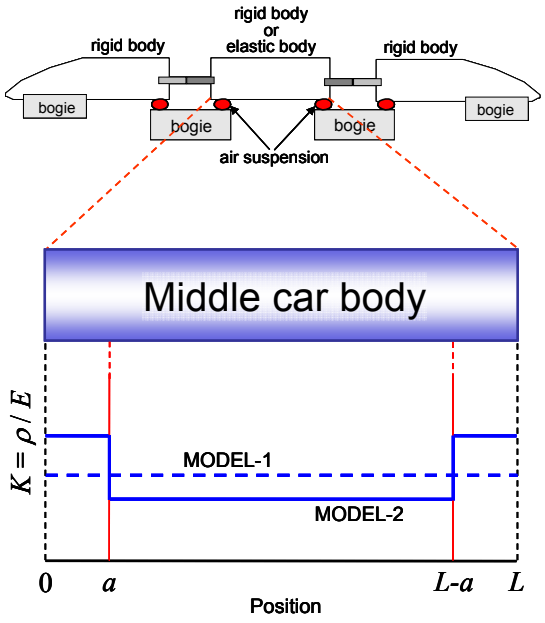

Figure 5: Elastic body models for the middle car body. A distribution of the parameter ρ/E is given in MODEL-2, while ρ/E is constant along the car body in MODEL-1.

Test results of bending-mode vibration of a maglev car body were reported (Takigami & Tomioka 2002). Experimental data of resonance frequencies of the first, second, and third bending modes are listed in Table 1. Two kinds of experiments were performed: a stationary test and a running test. In the stationary test the middle car was fixed by air springs and forced to vibrate in the vertical direction.

Bending-mode resonance frequencies obtained with MODEL-1 are shown in Table 1. Although resonance frequencies can be changed by adjusting the parameter E, the frequency ratios cannot be changed. No good analysis model was obtained from MODEL-1. On the other hand, MODEL-2 gave an acceptable analysis model, which had the resonance frequencies shown in Table 1. This model was obtained by selecting the parameters as listed in Table 2.

In the vehicle dynamics analysis, the same elastic vibration characteristics were assumed in the lateral direction as those in the vertical direction.

Table 1: Resonance frequencies of vertical bending modes.

Mode	JR tests		Analysis models	
	Stationary	Running	MODEL-1	MODEL-2
1	13.8 (1)	11.6 (1)	3.9 (1)	10.5 (1)
2	24.2 (1.8)	24.6 (2.1)	14.6 (3.7)	15.2 (1.4)
3	33.9 (2.5)	29.7 (2.6)	29.4 (7.5)	26.3 (2.5)

Unit: Hz, (Frequency ratio normalized by fundamental frequency)

Table 2: Model parameters obtained from MODEL-2.

Length (m)	24.3
Radius (m)	2.052
Number of nodes	37
a (m)	3.275
Modulus of longitudinal elasticity E (End) (N/m^2)	4.0×10^7
Modulus of longitudinal elasticity E (Middle) (N/m^2)	3.0×10^7
Mass density ρ (End) (kg/m^3)	90
Mass density ρ (Middle) (kg/m^3)	16.96
Poisson ratio	0.3

4 NUMERICAL ANALYSIS RESULTS

Numerical analysis of the vehicle dynamics were carried out. Both the rigid model and the elastic model of the car body, which were discussed in the previous section, were applied. The results obtained with these models are shown and compared in this section. The following two guideway conditions were applied:

(1) Straight guideway with imperfections of levitation coil arrangement or panel arrangement, and

(2) Curve guideway of 8,000 m in radius.

Vehicle dynamics characteristics are discussed below from the acceleration spectrum at the centre of gravity of the middle car.

4.1 Straight guideway with imperfections

Figure 6 shows numerical analysis results of vertical and lateral vibration accelerations of the middle car body when the vehicle moves at 500 km/h along a straight guideway with random errors in eight-figured levitation coil arrangement. The errors were random and smaller than 5 mm. There are peaks around 1.2 Hz and 4.6 Hz in Figure 6 (a) and 1.2 Hz and 6.2 Hz in Figure 6 (b), which are the resonance frequencies of secondary suspensions. Peaks around 11 Hz and 28 Hz are caused by the elastic vibration of the first mode and third mode, respectively. The amplitude of the elastic vibration is larger in the lateral direction than in the vertical direction, and almost proportional to the amount of coil irregularities in the range below about 5 mm.

Figure 7 shows vertical and lateral vibration accelerations when the vehicle moves at 500 km/h along a straight guideway with random errors in panel arrangement. The errors were smaller than 5 mm. Although in the results obtained with the elastic model the peaks around 4.6 Hz in Figure 7 (a), around 6.2 Hz in Figure 7 (b), and 11 Hz and 28 Hz in both figures are slightly increased, the elastic vibration has only a limited effect.

The frequencies of perturbing electromagnetic force range up to higher than 100 Hz in the imperfections in coil arrangement and up to about 5 Hz in those in panel arrangement. Therefore, the imperfections in coil arrangement strongly influence the elastic vibration of the middle car body, while those in panel arrangement quite slightly do it.

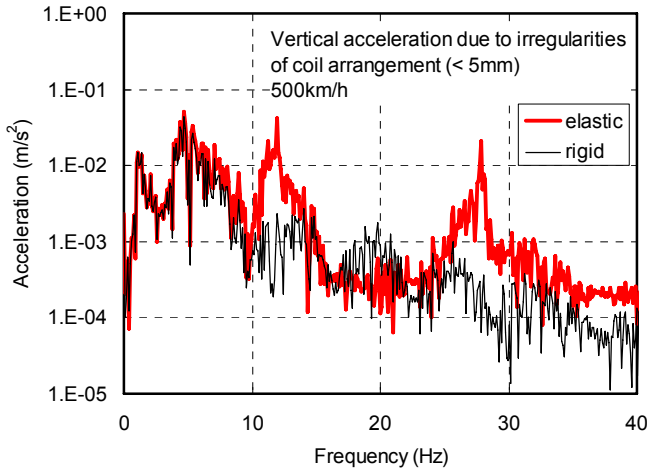

(a) Vertical vibration acceleration

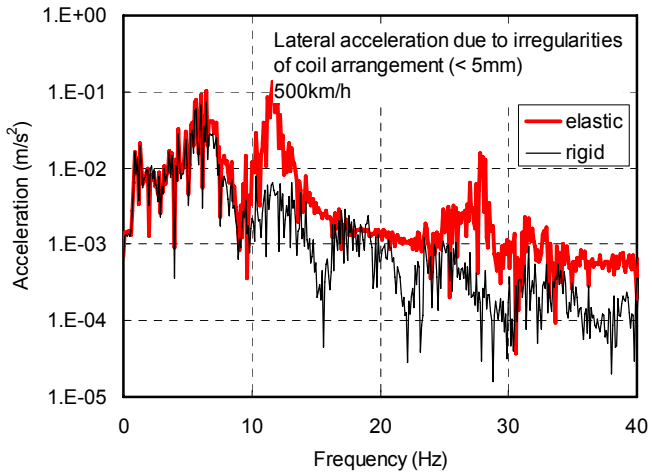

(b) Lateral vibration acceleration

Figure 6: Influence of coil arrangement imperfections. Spectrum of vertical and lateral vibration acceleration of the vehicle moving at 500 km/h along a straight guideway with imperfections (< 5mm) of coil arrangement.

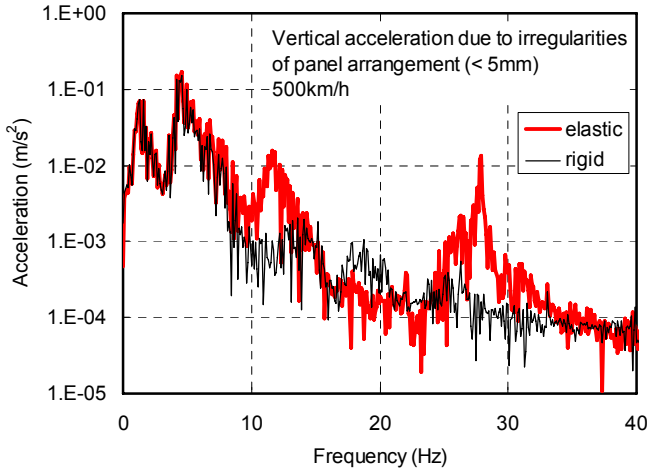

(a) Vertical vibration acceleration

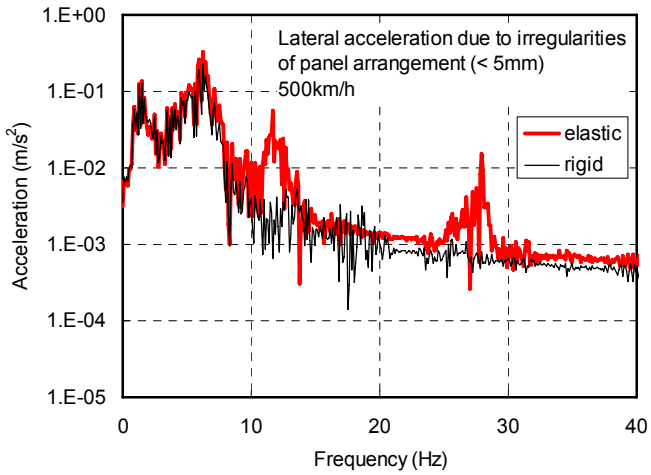

(b) Lateral vibration acceleration

Figure 7: Influence of guideway panel arrangement imperfections. Spectrum of vertical and lateral vibration accelerations of the vehicle moving at 500 km/h along a straight guideway with imperfections (< 5mm) of guideway panel arrangement.

4.2 Vibration of vehicle moving along a curve

As another simulation condition, a curve with a radius of 8,000 m and a cant angle of 0.1745 rad was applied as shown in Figure 8. Continuous movement along the curve, namely movement along the circle with a radius of 8,000 m was assumed. There were no easement curve sections along the curve. The panel structure of the ground coils for propulsion, levitation and guidance shown in Figure 8 (a) causes the oscillating electromagnetic force. The length of each panel is 12.6 m. A frequency calculated from the panel length of 12.6 m and the vehicle speed of 500 km/h is about 11.0 Hz.

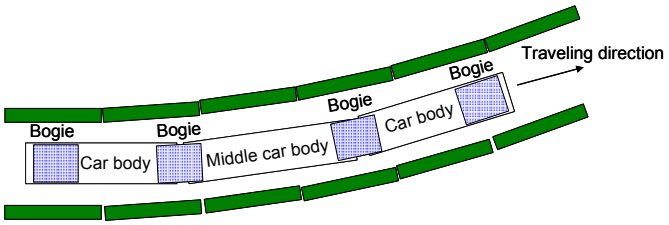

(a) Top view

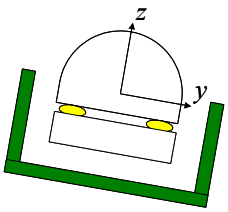

(b) Cross section and *y*-*z* coordinate

Figure 8: Model of the guideway panels and the vehicle moving along the curve.

Figure 9 shows numerical analysis results of vertical and lateral vibration accelerations at the center of gravity of the middle car body when the vehicle moves along the curve at 400 or 500 km/h. Acceleration spectrums obtained with the rigid and elastic models are compared.

Figures 9 (a) and 9 (b) show the vertical and lateral vibration accelerations for 500 km/h. There were peaks around 11 Hz, which is the main frequency of the perturbing electromagnetic force from the panels, in both vertical and lateral accelerations. The elasticity of the middle car body causes the increase of the peak around 11 Hz by about one order of magnitude, because 11 Hz is near the resonance frequency of the first-mode vibration of the elastic car body. The acceleration around 11 Hz of elastic lateral vibration causes the considerable deterioration of riding comfort.

Figure 9 (c) shows the lateral vibration acceleration for 400 km/h. There were peaks around 8.8 Hz, which is the main frequency of the perturbing electromagnetic force from the panels. This frequency is slightly off the resonance frequency of elastic vibration. The increase of the amplitude from that obtained with the rigid model at the peak is not so much as that for 500 km/h.

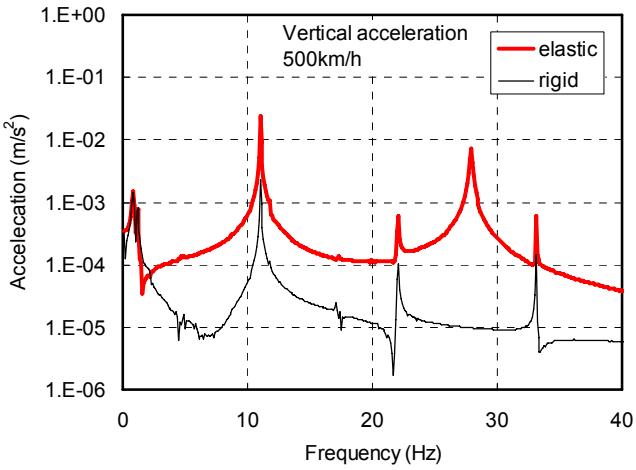

(a) Vertical vibration acceleration at 500 km/h

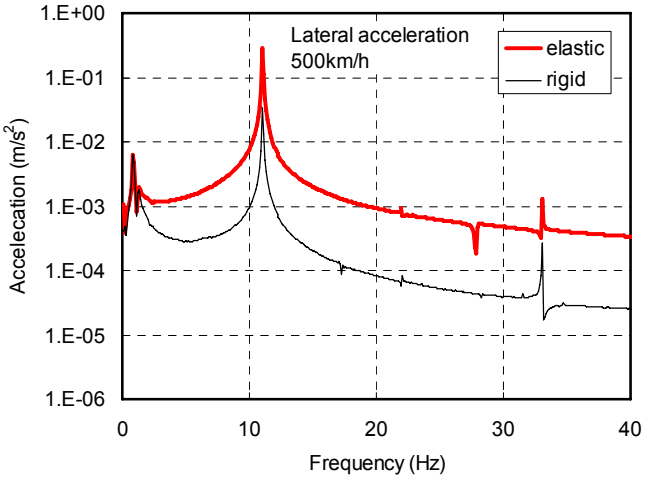

(b) Lateral vibration acceleration at 500 km/h

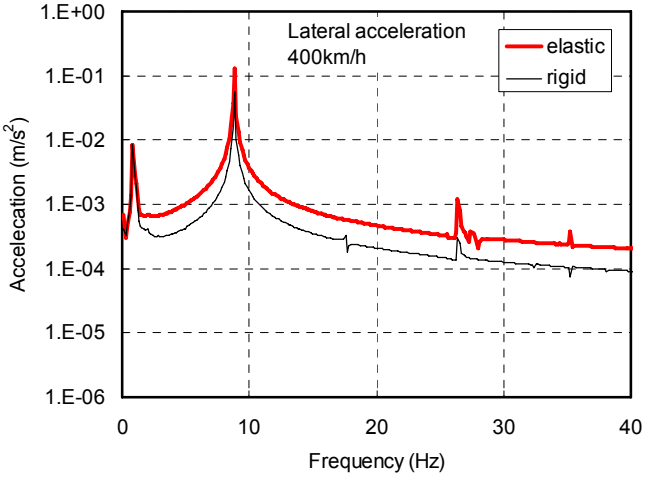

(c) Lateral vibration acceleration at 400 km/h

Figure 9: Comparison of spectrums of vertical or lateral vibration acceleration between the rigid model and the elastic model of the vehicle moving along the curve at 400 or 500 km/h.

The amplitude of vibration was below 1 mm for vertical motion and below 2 mm for lateral motion, which will not cause any problems during vehicle movement. The car bodies used at Yamanashi Maglev Test Line have higher elastic resonance frequencies and have no serious problems mentioned above at speeds up to around 500 km/h.

The developed simulation tools and models will be used for future numerical analysis of vehicle dynamics and riding comfort where elastic vibrations have essential effects.

5 CONCLUSIONS

This paper discussed the elastic body models of superconducting maglev vehicles for numerical analysis of vehicle dynamics and riding comfort. The elastic cylindrical beam model was created, and then numerical simulations of vehicle dynamics of the maglev train were carried out, where the vehicle moved along the straight guideway with imperfections of coil or panel arrangement, or along the curve with a radius of 8,000 m. The results showed that the influence of elastic vibration became larger when larger perturbation force was applied to the vehicle. In particular, rather large vibration occurred in the transient phase when the perturbation forces due to guideway imperfections were resonant with the elastic bending modes of the vehicle.

REFERENCES

Early, R. & Ohsaki, H. 2001. Numerical simulation of the vehicle dynamics of the superconducting Maglev system incorporating the LSM data interpolation method. *The Third International Symposium on Linear Drives for Industry Applications (LDIA2001), Nagano, 17-19 October 2001*: 186-191.

Early, R., Abe, Y. & Ohsaki, H. 2002. Numerical analysis of the vehicle dynamics of the superconducting maglev system at the Yamanashi test line, *The 17th International Conference on Magnetically Levitated Systems and Linear Drives (Maglev 2002), Lausanne, 3-5 September 2002*. PP05301.

Fujiwara, S. & Fujimoto, T. 1989. Characteristics of the combined levitation and guidance system using ground coils on the side wall of the guideway. *The 11th International Conference on Magnetically Levitated Systems and Linear Drives (Maglev '89), Yokohama, 7-11 July 1989*: 241-244.

Ohsaki, H. Early, R. & Suzuki, E. 2000. Numerical simulation of the vehicle dynamics of the superconducting Maglev system. *The 16th International Conference on Magnetically Levitated Systems and Linear Drives (Maglev'2000), Rio de Janeiro, 7-10 June 2000*: 230-235.

Ohsaki, H. & Abe, Y. 2003. Numerical simulation of vehicle dynamics of the superconducting maglev system using an elastic vehicle model, *The 4th International Symposium on Linear Drives for Industry Applications (LDIA 2003), Birmingham, 8-10 September 2003*. 191-194.

Seki, A., Tsuruga, H., Inoue, A., Kaminishi, K., Mizutani, T. & Furuki, T. 2002. The status of the development and the running tests of the JR-Maglev. *The 17th International Conference on Magnetically Levitated Systems and Linear Drives (Maglev 2002), Lausanne, 3-5 September 2002*: PP01109.

Takigami, T. & Tomioka, T. 2002. Elastic vibration characteristics of recent light-weight vehicles. *RTRI Report (in Japanese)* 16 (5): 23–28.